Lab Course: Bell's Inequality and Quantum Tomography

Revision April 2020

Contents

Bell's Inequality & Quantum Tomography

Advanced Laboratory Course

Quantum mechanical systems exhibit fundamentally different properties compared to classical systems. While the state of a classical particle can at any time be described by a set of well defined classical variables, quantum particles can be in superposition of different sates. If two or more particles are in a superposition such that the full state of the system can only be described by a joint superposition, then these particles are called entangled. The question whether the behaviour of entangled systems is determined by classical (local, realistic) variables was posed in a well-known paper in 1935 by Albert Einstein, Boris Podolsky, and Nathan Rosen (collectively "EPR"). Later, Bell formulated an inequality which allows to experimentally test whether the behaviour of entangled particles can be explained using such classical variables.

Besides these fundamental physics questions, entanglement is the key element for applications of quantum physics such as quantum cryptography, teleportation or quantum computation. Furthermore, its characteristics can be used for a fundamental test of non-classical properties of quantum theory. Quantum tomography is an essential tool for many of these applications. In this lab course we will perform quantum state tomography on polarization-entangled photon pairs and violate Bell's inequality.

1 Qubits and entanglement

First of all, the theoretical framework of two-photon entangled states is described. Therefore, the basic properties of quantum mechanics are briefly summarized (for further details see, e.g., [1, 2]) and afterwards are adapted to two-photon entanglement.

1.1 Characterization of qubit states

1.1.1 What is a qubit?

In general, a state is described by a minimal set of physical quantities providing full information about the considered system. In classical mechanics the state of a physical system is completely characterized by the generalized coordinate $\vec{q}$ and the generalized momentum $\vec{p}$. In contrast, in quantum mechanics a physical state is given by a vector in an in general infinite-dimensional complex vector space - the Hilbert space [3].

In this lab course we consider the polarization degree of freedom of photons as our physical system. The Hilbert space of the polarization of a single photon has dimension two. Each polarization state can be written as the superposition of two basis vectors, e.g., the horizontal $|H\rangle$ and vertical $|V\rangle$ polarization. Thus, a general polarization state is given by

$$|\psi\rangle = a\,|H\rangle + b\,|V\rangle \mathrel{\widehat{=}} \begin{pmatrix} a \\ b \end{pmatrix} \text{ with } |a|^2 + |b|^2 = 1. \tag{1.1}$$

By ignoring a global phase and considering the normalization implicitly [4], this can be expressed as

$$|\psi_{\theta,\phi}\rangle = \cos\left(\frac{\theta}{2}\right)|H\rangle + e^{i\phi}\sin\left(\frac{\theta}{2}\right)|V\rangle \text{ with } \theta \in [0,\pi] \text{ and } \phi \in [0,2\pi). \tag{1.2}$$

Due to the quantum superposition principle any normalized linear combination of two states is a possible state again. In 1995 Schumacher established the word "qubit" for such two-level quantum states as the quantum mechanical analogue of the classical bit.

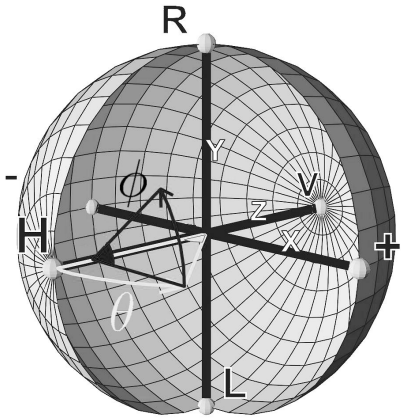

Figure 1.1: The Poincaré sphere represents the Hilbert space of one polarization encoded qubit. The eigenvectors of the Pauli matrices $(\widehat{\sigma}_x, \widehat{\sigma}_y, \widehat{\sigma}_z)$ are situated on the three orthogonal axis (X, Y, Z) (from [5]).

The full Hilbert space of a polarization-encoded qubit can be illustrated by the Poincaré sphere, as seen in figure 1.1. A pure state $|\psi\rangle$ is represented by a vector ending at the surface of the Poincaré sphere, while a mixed state lies within the sphere. The state $|\psi\rangle$ can be reached by rotating $|H\rangle$ by an angle θ around the Y axis and by ϕ around the Z axis.

In quantum mechanics a measurement is represented by observables, i.e., Hermitian operators [1]. More precisely, a (projective) measurement is defined as the projection onto one of the eigenstates of an observable and the measurement result is the corresponding eigenvalue. An example of operators acting on the 2-dimensional qubit Hilbert space are the Pauli spin matrices

$$\begin{aligned} \widehat{\sigma}_x &= \begin{pmatrix} 0 & 1 \\ 1 & 0 \end{pmatrix} = |H\rangle\langle V| + |V\rangle\langle H|\,, \\ \widehat{\sigma}_y &= \begin{pmatrix} 0 & -i \\ i & 0 \end{pmatrix} = i(|V\rangle\langle H| - |H\rangle\langle V|), \\ \widehat{\sigma}_z &= \begin{pmatrix} 1 & 0 \\ 0 & -1 \end{pmatrix} = |H\rangle\langle H| - |V\rangle\langle V|\,. \end{aligned} \tag{1.3}$$

Together with the identity matrix $\mathbb{1}_2$, these operators form a basis of the vector space of Hermitian operators acting on the two-dimensional qubit Hilbert space. Their eigenvectors are an orthogonal basis on the two-dimensional state space [5]. In figure 1.1 the basis of the Poincaré sphere is given by the eigenvectors of the Pauli spin matrices.

A measurement of a polarization qubit can be associated to two possible eigenvalues, $+1$ or -1, and the corresponding eigenvectors are defined using

$$\begin{aligned} \widehat{\sigma}_x \left[\frac{1}{\sqrt{2}}(|H\rangle \pm |V\rangle)\right] &= \widehat{\sigma}_x \ |+/-\rangle \ &= \pm \ |+/-\rangle\,, \\ \widehat{\sigma}_y \left[\frac{1}{\sqrt{2}}(|H\rangle \pm i\,|V\rangle)\right] &= \widehat{\sigma}_y \ |R/L\rangle \ &= \pm \ |R/L\rangle\,, \\ \widehat{\sigma}_z \ |H/V\rangle \ &= \pm |H/V\rangle\,. \end{aligned} \tag{1.4}$$

Here we use the short hand notation $|+/-\rangle$ for $\pm 45°$ linearly polarized light and $|R/L\rangle$ corresponding to right/left circular polarization.

A general observable $\widehat{\sigma}_{\theta,\phi}$ can be expressed in terms of the Pauli operators as

$$\widehat{\sigma}_{\theta,\phi} = \cos(\phi)\sin(\theta)\ \widehat{\sigma}_x + \sin(\phi)\sin(\theta)\ \widehat{\sigma}_y + \cos(\theta)\ \widehat{\sigma}_z, \tag{1.5}$$

for example

$$\begin{aligned} \widehat{\sigma}_{0,0} &= \widehat{\sigma}_z, \\ \widehat{\sigma}_{\frac{\pi}{2},0} &= \widehat{\sigma}_x, \\ \widehat{\sigma}_{\frac{\pi}{2},\frac{\pi}{2}} &= \widehat{\sigma}_y. \end{aligned} \tag{1.6}$$

Let us now consider a general state $|\psi_{\theta,\phi}\rangle$. Assume we want to measure the $|H\rangle$ component of this state, so we want to perform a projection using the operator

$$P_H = |H\rangle\langle H| = \frac{1}{2}(\mathbb{1} + \widehat{\sigma}_z). \tag{1.7}$$

The probability of occurrence for this projection can be calculated as the expectation value of the projector P_H via

$$\langle\psi_{\theta,\phi}|P_H|\psi_{\theta,\phi}\rangle = \cos^2\left(\frac{\theta}{2}\right). \tag{1.8}$$

A general projector $P^{\pm}_{\theta,\phi}$ is given by

$$P^{\pm}_{\theta,\phi} = |\psi_{\theta,\phi}\rangle\langle\psi_{\theta,\phi}| = \frac{1}{2}(\mathbb{1} \pm \widehat{\sigma}_{\theta,\phi}). \tag{1.9}$$

With this, the single qubit correlation[1] for a pure state $|\psi\rangle$ can be calculated in a general basis setting $\widehat{\sigma}_{\theta,\phi}$

$$K(\theta,\phi) = \langle\psi|\widehat{\sigma}_{\theta,\phi}|\psi\rangle = \langle\psi|P^{+}_{\theta,\phi} - P^{-}_{\theta,\phi}|\psi\rangle = p^{+}_{\theta,\phi} - p^{-}_{\theta,\phi} \tag{1.10}$$

[1] The term "correlation" will be defined below in the context of 2-qubit systems, where it captures how parallel the measurement outcomes of two parties in the respective basis are. In the 1-qubit case, it measures how parallel the single qubit outcome is to the respective measurement basis. The 1-qubit ("local") correlations correspond to the elements of the Bloch vector of the single qubit. More on this later.

with the probabilities of occurrence $p^+_{\theta,\phi}$, $p^-_{\theta,\phi}$ [6].

1.1.2 Two-qubit states

So far we have considered the polarization of a single photon as implementation of a single qubit. In the experiment we will use two entangled qubits represented by two photons entangled in the polarization degree of freedom. The spatial separation of the two qubits as another degree of freedom allows us to distinguish them, i.e., the two qubits can be numbered.

In this section we want to describe this state theoretically. The system of the two qubits can be represented by a state in the corresponding Hilbert space $\mathcal{H}$. The latter is given by the tensor product of the two separate Hilbert spaces $\mathcal{H}_1$ and $\mathcal{H}_2$ spanning the vector space of each qubit [1], i.e.,

$$\mathcal{H} = \mathcal{H}_1 \otimes \mathcal{H}_2. \tag{1.11}$$

A basis of $\mathcal{H}$ can be obtained by defining the tensor product of the single qubit basis vectors[2] with

$$\begin{aligned} |\uparrow\uparrow\rangle &= |\uparrow\rangle \otimes |\uparrow\rangle\,, \quad |\uparrow\downarrow\rangle = |\uparrow\rangle \otimes |\downarrow\rangle\,, \\ |\downarrow\uparrow\rangle &= |\downarrow\rangle \otimes |\uparrow\rangle\,, \quad |\downarrow\downarrow\rangle = |\downarrow\rangle \otimes |\downarrow\rangle\,. \end{aligned} \tag{1.12}$$

So the most general two-qubit state in this basis is given by [6]

$$|\Psi(a_{\uparrow\uparrow}, a_{\uparrow\downarrow}, a_{\downarrow\uparrow}, a_{\downarrow\downarrow})\rangle = a_{\uparrow\uparrow}\,|\uparrow\uparrow\rangle + a_{\uparrow\downarrow}\,|\uparrow\downarrow\rangle + a_{\downarrow\uparrow}\,|\downarrow\uparrow\rangle + a_{\downarrow\downarrow}\,|\downarrow\downarrow\rangle \tag{1.13}$$

with $a_{\uparrow\uparrow}, a_{\uparrow\downarrow}, a_{\downarrow\uparrow}, a_{\downarrow\downarrow} \in \mathbb{C}$ and $|a_{\uparrow\uparrow}|^2 + |a_{\uparrow\downarrow}|^2 + |a_{\downarrow\uparrow}|^2 + |a_{\downarrow\downarrow}|^2 = 1$.

States that can be directly expressed as a tensor product of single qubit states are called separable or product states, for example

$$|\Psi\rangle_{\text{sep}} = |\uparrow\uparrow\rangle\,. \tag{1.14}$$

Keep in mind that any superposition of these states is also an element of the Hilbert space $\mathcal{H}$. States which cannot be written as a tensor product of single qubit states are called non-separable or entangled, for example

$$|\Psi\rangle_{\text{ent}} = \frac{1}{\sqrt{2}}(|\uparrow\uparrow\rangle + |\downarrow\downarrow\rangle). \tag{1.15}$$

In order to characterize two-photon states, observables acting on the two-qubit vector space have to be described. Let $\widehat{A}_1$ and $\widehat{A}_2$ be observables acting on $\mathcal{H}_1$ and $\mathcal{H}_2$, respectively. Their tensor product $\widehat{A}_1 \otimes \widehat{A}_2$ is the observable acting on $\mathcal{H}$, defined by

$$[\widehat{A}_1 \otimes \widehat{A}_2]\,[|\psi_1\rangle \otimes |\psi_2\rangle] \;=\; [\widehat{A}_1\,|\psi_1\rangle] \otimes [\widehat{A}_2\,|\psi_2\rangle] \text{ with } \psi_1 \in \mathcal{H}_1 \text{ and } \psi_2 \in \mathcal{H}_2. \tag{1.16}$$

Any of these observables can be formed by a linear combination of tensorially multiplied Pauli matrices,

$$\widehat{A}_1 \otimes \widehat{A}_2 = \sum_{i,j=0}^{3} s_{ij}\;\widehat{\sigma}_i \otimes \widehat{\sigma}_j \tag{1.17}$$

[2] In the following, a general notation $\{|\uparrow\rangle, |\downarrow\rangle\}$ is used. In specific situations it could represent a polarization basis such as $\{|H\rangle, |V\rangle\}$, $\{|+\rangle, |-\rangle\}$ or $\{|R\rangle, |L\rangle\}$.

with $\widehat{\sigma}_0 = \mathbb{1},\ \widehat{\sigma}_1 = \widehat{\sigma}_x,\ \widehat{\sigma}_2 = \widehat{\sigma}_y,\ \widehat{\sigma}_3 = \widehat{\sigma}_z$ and $s_{i,j} \in \mathbb{C}$.

Using the tensor product, two-qubit projectors can be defined similarly to the single qubit case. For example, the P_{HV} projector is given by

$$P_{HV} = P_H \otimes P_V = \frac{1}{2}(\mathbb{1} + \widehat{\sigma}_z) \otimes \frac{1}{2}(\mathbb{1} - \widehat{\sigma}_z). \tag{1.18}$$

The ZZ correlation, i.e., the correlation of the measurement results when both qubits are measured in their respective Z basis, corresponds to the expectation value of the observable $\widehat{\sigma}_z \otimes \widehat{\sigma}_z$. For the state $|\Psi(a_{HH}, a_{HV}, a_{VH}, a_{VV})\rangle$, the expectation value of $\widehat{\sigma}_z \otimes \widehat{\sigma}_z$ is given by [5]

$$\begin{aligned} K_{zz} &= \langle\Psi(a_{HH}, a_{HV}, a_{VH}, a_{VV})|\widehat{\sigma}_z \otimes \widehat{\sigma}_z|\Psi(a_{HH}, a_{HV}, a_{VH}, a_{VV})\rangle = \\ &= \frac{1}{4}(\langle\Psi|[\mathbb{1} + \widehat{\sigma}_z] \otimes [\mathbb{1} + \widehat{\sigma}_z]|\Psi\rangle - \langle\Psi|[\mathbb{1} + \widehat{\sigma}_z] \otimes [\mathbb{1} - \widehat{\sigma}_z]|\Psi\rangle \\ &- \langle\Psi|[\mathbb{1} + \widehat{\sigma}_z] \otimes [\mathbb{1} - \widehat{\sigma}_z]|\Psi\rangle + \langle\Psi|[\mathbb{1} - \widehat{\sigma}_z] \otimes [\mathbb{1} - \widehat{\sigma}_z]|\Psi\rangle) = \\ &= \langle\Psi|P_H \otimes P_H|\Psi\rangle - \langle\Psi|P_H \otimes P_V|\Psi\rangle - \langle\Psi|P_V \otimes P_H|\Psi\rangle + \langle\Psi|P_V \otimes P_V|\Psi\rangle = \\ &= |a_{HH}|^2 - |a_{HV}|^2 - |a_{VH}|^2 + |a_{VV}|^2 = p_{HH} - p_{HV} - p_{VH} + p_{VV}, \end{aligned} \tag{1.19}$$

where p_{ij} $(i, j \in \{H, V\})$ are the probabilities of occurrence in the $|H/V\rangle$ basis. A correlation value $K_{zz} = +1$ implies that the measurement outcomes of both qubits are always equal, i.e., the state is correlated in this basis. An uncorrelated result is expressed by $K_{zz} = 0$, while an anticorrelated result corresponds to $K_{zz} = -1$.

1.1.3 Bell States and entanglement

In this section, different entangled states are considered in more detail. The four Bell states are examples of maximally entangled two-qubit states. They are defined as

$$\begin{aligned} |\phi^+\rangle &= \frac{1}{\sqrt{2}}\left(|HH\rangle + |VV\rangle\right), \\ |\phi^-\rangle &= \frac{1}{\sqrt{2}}(|HH\rangle - |VV\rangle), \\ |\psi^+\rangle &= \frac{1}{\sqrt{2}}(|HV\rangle + |VH\rangle), \\ |\psi^-\rangle &= \frac{1}{\sqrt{2}}(|HV\rangle - |VH\rangle). \end{aligned} \tag{1.20}$$

The mathematical property that they cannot be produced by only a single tensor product of local states has profound consequences in the context of quantum mechanics [3]. Some properties arising from this effect are

1. Each Bell state can be converted to any other Bell state by a unitary transformation on one of the two qubits [5],

$$|\phi^+\rangle = (\mathbb{1} \otimes \widehat{\sigma}_z)\,|\phi^-\rangle = (\mathbb{1} \otimes \widehat{\sigma}_x)\,|\psi^+\rangle = (\mathbb{1} \otimes \widehat{\sigma}_y)\,|\psi^-\rangle \tag{1.21}$$

   up to a global phase. So a transformation on only one qubit of an entangled state changes the complete state. This becomes even more interesting, when considering

that the new state is rotated back to the original one by a transformation on the other qubit. For example,

$$|\phi^+\rangle \rightarrow (\mathbb{1} \otimes \widehat{\sigma}_x)\,|\phi^+\rangle = |\psi^+\rangle\,, \tag{1.22}$$
$$|\psi^+\rangle \rightarrow (\widehat{\sigma}_x \otimes \mathbb{1})\,|\psi^+\rangle = |\phi^+\rangle\,. \tag{1.23}$$

2. Entangled states are correlated in more than one basis, in contrast to separable states. For the latter, a (maximal) correlation can only be observed in one specific two-photon basis, whereas in other bases (orthogonal to the basis of maximal correlation) they are uncorrelated. A reverse result occurs, if one considers local correlations calculated in the basis $\widehat{\sigma}_i \otimes \mathbb{1}$ ($i \in \{X, Y, Z\}$). They vanish for maximally entangled states making it impossible to determine the single photon state independently of the other photon state. In contrast, both qubits of a 2-qubit product state can be described locally. certainty. For example,

$$\begin{aligned} &\langle HH|\widehat{\sigma}_z \otimes \mathbb{1}|HH\rangle = 1, \\ &\langle \phi^+|\widehat{\sigma}_i \otimes \mathbb{1}|\phi^+\rangle = 0 \quad \text{with } i \in \{x, y, z\}. \end{aligned} \tag{1.24}$$

These properties give rise to violation of local realism because for a local-realistic theory the measurement of one particle, which is spatially separated from another one, cannot influence the second particle. This will be described more precisely in the next section.

1.2 EPR paradox and Bell's inequality

1.2.1 EPR paradox

The Copenhagen interpretation of quantum mechanics leads to intrinsic random results for measurements. Therefore, Einstein was convinced that "the description of reality as given by a wave function is not complete" [7]. Especially, the uncertainty principle, which prohibits the possibility to measure two non-commuting operators with unlimited accuracy, irritated Einstein. He assumed that it should be possible to find a local theory with hidden parameters explaining the results of quantum theory, but still fulfilling the requirements of a deterministic and local theory. So in 1935 Einstein, Podolski and Rosen (EPR) published a gedankenexperiment which should demonstrate the existence of hidden variables and the incompleteness of quantum mechanics. The basic assumptions (formulated in the version of Bohm and Aharonov) can be summarized as

1. **Completeness:** "Every element of the physical reality must have a counterpart in the physical theory." [7]

2. **Realism:** "If, without in any way disturbing a system, we can predict with certainty (i.e., with probability equal to unity) the value of a physical quantity, then there exists an element of physical reality corresponding to this physical quantity." [7]

3. **Locality:** It is possible to separate physical systems so that they do not influence each other, as they cannot transmit information with v > c.

4. **Perfect Anticorrelations:** If you measure the spin of both particles in the same direction, you will get opposite results.

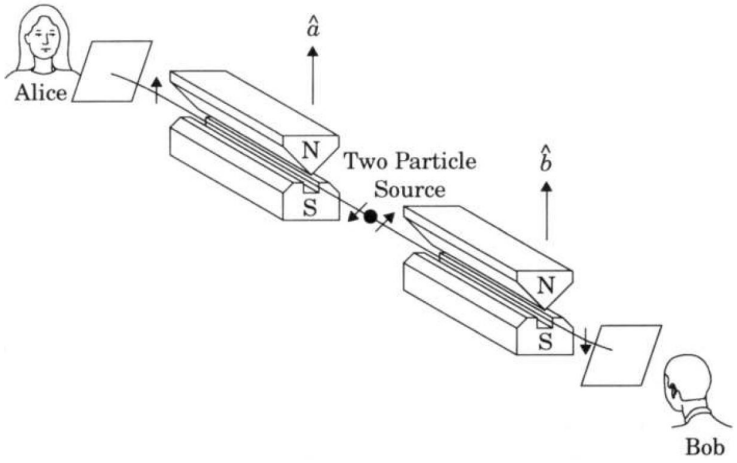

Figure 1.2: Stern-Gerlach experiment for the determination of spins of two particles (from [8]).

They considered two spin-$\frac{1}{2}$ particles in an entangled state $|\psi\rangle = \frac{1}{\sqrt{2}}(|\uparrow\downarrow\rangle + |\downarrow\uparrow\rangle)$ (see the Bell state $|\psi^+\rangle$ of Eqn.1.20) which fly away in different directions [9]. By a spin measurement of particle A, e.g., along the X direction, the spin of particle B can also be determined along this direction. Due to assumption 3. this measurement does not influence particle B and due to 4., the spin of particle B is opposite to particle A's spin. So the spin in X direction of particle B is known and due to 2., it is an element of physical reality. It would also be possible to measure the spin of particle B, e.g., along the Z direction and thus, this spin is also an element of physical reality. This result contradicts the uncertainty principle. Therefore, as they claim, hidden variables must exist which determine these measurement results being necessary to extend quantum mechanics to a complete, local and realistic theory.

Bohr countered that knowing the state of a whole system does not necessarily mean that its parts can be determined, as they are not in a defined state. Furthermore, after the measurement of one particle the result of the other one will instantaneously be known. This is a contradiction to the locality assumption when the two particles are spatially separated. So Bohr's version explained the problem by rejecting the principles of local realism.

The EPR-paradox became more a philosophical problem during nearly the next 30 years (see also [10]). No possibility had been known to measure a difference between the predictions of quantum mechanics and those of a local hidden variable theory.

1.2.2 Bell's inequality and CHSH inequality

In 1964 Bell found a solution for this problem [11]. He showed that quantum mechanics and local hidden variable theories give different predictions for certain measurements. In more detail, under the assumptions of locality and realism, one can find an inequality that must be necessarily satisfied by correlations between outcomes of measurements performed on

distant particles. On the other hand, in the realm of quantum mechanics, Bell's inequality can be violated if the particles are entangled.

In contrast to the original proposal of Bell, in this experiment a similar inequality formulated by Clauser, Horne, Shimony and Holt (CHSH) is used [12]. As the CHSH inequality does not require perfect correlations, it is better adapted to realistic experimental conditions. For an exact derivation of the CHSH inequality, see [13]. Here only a short conclusion is given.

Local-realistic description

We consider the setup as described for the EPR-paradox. Let λ be the set of hidden variables (without loss of generality it should be one dimensional) and $p(\lambda)$ its probability distribution determining the measurement results for any possible measurement setting. Two different measurement outcomes are provided for particle A by $\{A(a,\lambda),\ A(a',\lambda)\}$ and for particle B by $\{B(b,\lambda),\ B(b',\lambda)\}$, where a, a' and b, b' are adjustable apparatus parameters. The measurement results are deterministic functions, i.e., they depend on λ and their spectrum is $\{\pm 1\}$. The principle of locality requires $A(a,\lambda)$ and $A(a',\lambda)$ to be independent from $B(b,\lambda)$ and $B(b',\lambda)$. This is ensured by a spatial separation of the measurement apparatuses. Consequently, the correlation value[3] E of the measurements factorizes as

$$E(a,b) = \int d\lambda\ p(\lambda)\ A(a,\lambda)\ B(b,\lambda) = E(a)\cdot E(b). \tag{1.25}$$

Taking into account the assumptions made so far and considering the possible values for the mesaurement outcomes, an equality for the different settings can be defined [3]. For a single measurement it is given by

$$\begin{aligned} &|A(a,\lambda)B(b,\lambda) - A(a,\lambda)B(b',\lambda)| + |A(a',\lambda)B(b,\lambda) + A(a',\lambda)B(b',\lambda) = \\ &\quad = \underbrace{|A(a,\lambda)}_{\begin{array}{c}\pm 1\\ \\ \end{array}}\underbrace{(B(b,\lambda) - B(b',\lambda))|}_{\begin{array}{c}0\\ \pm 2\\ 0\end{array}} + \underbrace{|A(a',\lambda)}_{\begin{array}{c}\pm 1\\ \\ \end{array}}\underbrace{(B(b,\lambda) + B(b',\lambda))|}_{\begin{array}{c}+2\\ 0\\ -2\end{array}} = 2. \end{aligned} \tag{1.26}$$

With the definition of the correlation value and the inequality $|\int f(x)dx| \leq \int |f(x)|dx$, one finally obtains the CHSH inequality

$$S(a,a',b,b') = |E(a,b) - E(a,b')| + |E(a',b) + E(a',b')| \leq 2. \tag{1.27}$$

Quantum violation

In quantum mechanics, the correlation functions can be calculated as described in the following [4]. As an example for the quantum violation of the Bell's inequality, we consider here the maximally entangled state (see Eqn.1.20)

$$|\phi^+\rangle = \frac{1}{\sqrt{2}}(|HH\rangle + |VV\rangle). \tag{1.28}$$

[3] Please note that the correlation function is for historical reasons denoted by E here. In the following, we will come back to denoting a correlation by the letter K.

The maximum violation of the CHSH inequality occurs for certain measurement settings. For the state $|\phi^+\rangle$ a maximal violation can be observed when measuring $\widehat{\sigma}_{\theta,\phi}$ of Eqn. 1.5 with

$$\begin{aligned} &\phi = 0 \text{ (for all measurements)} \\ &\theta_1 = \alpha = \frac{\pi}{2} \; ; \; \theta_2 = \alpha' = 0 \; ; \; \theta_3 = \beta = \frac{\pi}{4} \; ; \; \theta_4 = \beta' = -\frac{\pi}{4}. \end{aligned} \tag{1.29}$$

Note that a value of $\phi = 0$ corresponds to a rotation in the equatorial plane of the Bloch sphere. Hence, we here only need to consider states of linearly polarized light (see figure 1.1).

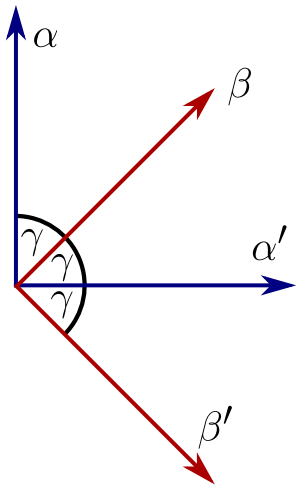

Figure 1.3: Illustration of the angles corresponding to maximal violation of the CHSH inequality where $\gamma = \frac{\pi}{4}$ (from [14]). Bob's measurement directions (red) are rotated compared to Alice's (blue).

The correlation function of the outcomes of both qubits depending on the respective angles α and β is found to be

$$E_{QM}(\alpha, \beta) = \langle \phi^+ | \widehat{\sigma}_{\alpha,0} \otimes \widehat{\sigma}_{\beta,0} | \phi^+ \rangle = \cos(\alpha - \beta). \tag{1.30}$$

With the above angles, one obtains

$$E_{QM}(\alpha, \beta) = E_{QM}(\alpha', \beta) = E_{QM}(\alpha', \beta') = -E_{QM}(\alpha, \beta') = \cos\left(\frac{\pi}{4}\right) = \frac{1}{\sqrt{2}}. \tag{1.31}$$

In the next step these values can be inserted in Eqn. 1.27, leading to a violation of the classical limit with

$$S_{QM}(\alpha, \alpha', \beta, \beta') = 2\sqrt{2} > 2. \tag{1.32}$$

The challenge of the loophole-free Bell test

In the decades following the discovery of Bell's inequality, experimentalists performed increasingly sophisticated tests of its violation. The first one was done by Freedman and Clauser in 1972 [15] and subsequently most prominently by A. Aspect et al. in 1981 and 1982 [16, 17]. But although these experiments resulted from great efforts for that time, they were far from ideal. Due to technological constraints, until 2015 all the experiments required additional assumptions to obtain a contradiction to local realism, affirming the quantum mechanical predictions up to the closure of different loopholes. Whenever a loophole is left opened, it allows for a local-realistic explanation of the measured data.

Two major loopholes exist [18]. The first one is the so called "locality loophole". It occurs, whenever the communication between the measurement settings of the two observers cannot be excluded before completing the actual measurement process. In experiments, this loophole can be ruled out by achieving a space-like separation of the two particles with respect to their measurement time. In 1998 the first experiment which violated a Bell's inequality under strict locality conditions has been performed by Weihs et al. [19] and was improved further by Scheidl et al. in 2010 [20], who separated the two observers by a distance of 144 km.

However, in all these experiments the detection efficiencies of the entangled photons were too low to close the so-called "detection loophole". This describes the possibility that the whole ensemble may behave according to local realism, while the detected particles do not because they are not representative for the whole ensemble. A Bell test, which eliminated successfully this loophole, was performed with a pair of entangled beryllium ions. But in this system the separation of the ions by a distance of about 3 μm gave no chance to close the locality loophole [4].

A Bell test that closes all experimental loopholes simultaneously (commonly referred to as loophole-free Bell test[4]) was first performed in 2015 by Hensen et al. [21], using electronic spins associated with a single defect center in diamonds separated by 1.3 km. The detection loophole was avoided thanks to the efficient spin read-out, while the use of fast random-basis selection and the spatial separation closed the locality loophole.

Two more loophole-free Bell test were reported in the same year by Giustina et al. [22] and by Shalm et al. [23]. They both used photonic systems with rapidly switching polarizers located far enough from the source to close the locality loophole and high-efficiency photon detectors to close the detection loophole.
In 2017 a fourth loophole-free Bell test was performed in a collaboration between LMU and MPQ [24] using entangled spin states of atoms separated by a distance of 398 m. Since the measurement result was reported every time the successful distribution of entanglement to the observers was confirmed, no detection loophole was opened at all. On the other hand, the locality loophole was closed by employing fast and efficient measurements of the atomic spin states at a sufficient distance together with fast quantum random number generators for selection of the measurement basis.

The importance of loophole-free observations of a violation of Bell's inequality stays

[4]Note that no experiment, as ideal as it is, can be said to be totally loophole-free.

in the strong support provided for the idea that nature cannot be described within the framework of local realism.

1.3 Density operator

So far, we have only considered pure states, which are represented by a state vector. However, such a state cannot be produced perfectly in an experiment. For example, because of uncontrollable, systematical changes of the state only incomplete information about the state can be extracted and therefore only probability statements are possible. In the density operator formalism the state can be described following the axioms of classical probability calculation.

1.3.1 Definition and general characteristics

Definition

The density operator [1] of any state is defined by

$$\rho = \sum_i p_i \left|\phi_i\right\rangle \left\langle\phi_i\right| \text{ with } \sum_i p_i = 1 \text{ and } \left|\phi_i\right\rangle \text{ being pure states.} \tag{1.33}$$

If among those pure states there exist a $|\phi_i\rangle$ for which $p_i = 1$ then ρ is a pure state with $\rho = |\phi_i\rangle \langle\phi_i|$ for that particular i. On the other hand, more than one pure state contributes in the above sum, the p_i are statistically distributed and the state is a *statistical mixture* over pure states. Such a state is therefore called a mixed state.

Conditions for density operators

The operator ρ is a density operator if and only if

- $\mathrm{Tr}(\rho) = 1$ (Probability conservation),
- $\rho \geq 0$ (ρ must be a positive semi-definite operator to describe a physical state, i.e., $\lambda_i \geq 0\ \forall i$ where λ_i are the eigenvalues of ρ),
- $\rho = \rho^\dagger$ (Hermitianity).

Representations

1. **Matrix representation**
   Consider a quantum ensemble of size N with occupancy numbers n_1, n_2,..., n_k corresponding to the orthonormal states $|1\rangle$, $|2\rangle$,..., $|k\rangle$, respectively, where $n_1 + n_2 + ... + n_k = N$. The density operator can be written as a matrix for a given orthonormal basis with
   $$\rho_{ij} = \langle i|\rho|j\rangle \tag{1.34}$$
   where i, $j \in \{1, 2, ..., N\}$ and $|i\rangle$, $|j\rangle$ being basis vectors.

2. **Pauli spin matrices representation**
   The density matrix can also be expressed through the Pauli spin matrices (see Sec. 1.1.1 and [25]). For a single qubit it is given as

$$\rho = \frac{1}{2} \sum_{i=0}^{3} s_i \, \widehat{\sigma}_i. \tag{1.35}$$

   Extending this formalism to two qubits (see Sec. 1.1.2) gives the parametrization

$$\rho = \frac{1}{2^2} \sum_{i,j=0}^{3} s_i \, \widehat{\sigma}_i \otimes \widehat{\sigma}_j. \tag{1.36}$$

Physical interpretation

The measurement of a density matrix through quantum tomography is the second part of this lab course. Therefore, the physical interpretation of the matrix elements ρ_{ij} will be explained briefly. The example of the single qubit state $\rho_R = |R\rangle \langle R|$ is presented to illustrate the differences between the diagonal and non-diagonal elements of a density matrix expressed in the $|H\rangle$, $|V\rangle$ basis. Its density matrix reads

$$\rho_R = \frac{1}{2} \begin{pmatrix} 1 & -i \\ i & 1 \end{pmatrix} = \frac{1}{2}(\mathbb{1} + \widehat{\sigma}_y). \tag{1.37}$$

- The diagonal element ρ_{ii} represents the probability for observing the system in the basis state $|i\rangle$. Thus, it is called the "population" of the state $|i\rangle$ and is always a positive real number. In this case, both diagonal elements are $\rho_{11} = \rho_{22} = 1/2$. Hence, this state can be found to be $|H\rangle$ or $|V\rangle$ with 50% probability each.

- The non-diagonal element ρ_{ij} (for $i \neq j$) describes the quantum coherences between the basis states $|i\rangle$ and $|j\rangle$. It does not vanish if the state $|\psi\rangle$ is a coherent linear superposition of $|i\rangle$ and $|j\rangle$. More precisely, for product states a set of basis transformations exists, acting individually on the subspaces $|i\rangle$ and $|j\rangle$, such that ρ takes diagonal form in the new product basis. Consequently, the non-diagonal elements have no invariant meaning for product states. Nevertheless, no product basis describes an entangled state and therefore ρ of an entangled state can never be diagonal in such a product basis. They are called "coherences" and are in general complex numbers [26]. In this particular example, the coherences are $\pm i/2$, indicating that the basis states have to be coherently superposed with the corresponding phase to result in the given state.

1.3.2 Applications of the density operator

All quantities which characterize a quantum state can be calculated out of a density matrix. Here some of these will be presented.

1. **Purity**
   The Purity describes if a state is pure or mixed,

$$\mathcal{P}(\rho) = \mathrm{Tr}(\rho^2). \tag{1.38}$$

   It is 1 for pure states and $1/N^2$ for a totally mixed N-qubit state [27].

2. **Expectation value for an operator**
   Following the Born Rule, the expectation value for an operator A can be calculated as

$$\langle A \rangle = \langle \psi | A | \psi \rangle = \mathrm{Tr}(\rho A), \tag{1.39}$$

   where the first expression holds only if a pure state $|\psi\rangle$ is considered. The last expression is most general.

3. **Fidelity**
   Uhlmann introduced the fidelity in 1976 [28] to measure the overlap between two states ρ and σ. In general, it is given by

$$\mathcal{F}(\rho, \sigma) = (\mathrm{Tr}(\sqrt{\sqrt{\sigma}\rho\sqrt{\sigma}}))^2. \tag{1.40}$$

   Please note that $\sqrt{\sigma}$ is the matrix root defined as a matrix with $\sqrt{\sigma}\sqrt{\sigma} = \sigma$. The fidelity can be used to quantify how well an experimental imperfect state ρ resembles another general state σ. In our case the reference state is pure and therefore the fidelity simplifies to [29]

$$\mathcal{F}(\rho, \sigma) = \mathrm{Tr}(\sigma\rho) = \langle \psi | \rho | \psi \rangle \tag{1.41}$$

   with $\sigma = |\psi\rangle \langle \psi|$.

4. **Entanglement detection**
   Many fascinating quantum mechanical effects are based on entanglement, which is therefore a powerful building block of quantum theory. As a consequence, it is crucial in some situations to be able to prove that a given quantum state is entangled. For this purpose different methods have been proposed [30]. Some fundamental ones are presented here.

   a) **PPT-criterion and negativity**
      The Positive Partial Transpose (PPT) criterion allows to verify if a state is entangled if its density matrix is known [5]. The density matrix of a separable state ρ can be written as

$$\rho_{sep} = \sum_i p_i \, \rho_i^a \otimes \rho_i^b, \tag{1.42}$$

      where p_i are the probabilities of the admixtures of $\rho_i^a \otimes \rho_i^b$. The partial transpose with respect to part A of a matrix is defined by

$$\rho^{T_a} = \sum_i p_i \, (\rho_i^a)^t \otimes \rho_i^b, \tag{1.43}$$

where $(\rho_i^a)^t$ denotes transposition of ρ_i^a.

The **Peres-Horodecki Theorem** for a two-qubit Hilbert space says that

$$\rho \text{ separable} \quad \Leftrightarrow \quad \rho^{T_a} \geq 0. \tag{1.44}$$

For example, the partial transpose of the product state $|HH\rangle$ is again a physical state with $\rho_{HH}^{T_a} \geq 0$ as

$$\rho_{HH} = |HH\rangle \langle HH| \overset{PT}{\rightarrow} \rho_{HH}^{T_a} = |HH\rangle \langle HH| . \tag{1.45}$$

But if we start with an entangled two-qubit state, its partial transpose will not be a valid density matrix anymore, e.g.,

$$\begin{aligned} \rho_{\phi^+} = |\phi^+\rangle \langle \phi^+| &= \frac{1}{2}(|HH\rangle \langle HH| + |HH\rangle \langle VV| + |VV\rangle \langle HH| + |VV\rangle \langle VV|) \\ \overset{PT}{\rightarrow} \rho_{\phi^+\phi^+}^{T_a} &= \frac{1}{2}(|HH\rangle \langle HH| + |VH\rangle \langle HV| + |HV\rangle \langle VH| + |VV\rangle \langle VV|). \end{aligned} \tag{1.46}$$

The matrix of the partial transpose has a negative eigenvalue of $-\frac{1}{2}$, i.e., $\rho_{\phi^+}^{T_a} \ngeq 0$. For two-qubit systems (as for all systems with equal or less than 6 dimensions in total), the PPT criterion is a necessary and sufficient test of entanglement.

b) **Entanglement witness**
An entanglement witness is an operator that allows to detect entangled states. It can also be used to define the probability of having generated the desired entangled state [14].

Terhal Theorem: Consider a density operator ρ (with $\rho \geq 0$) acting on a finite Hilbert space $\mathcal{H}_1 \otimes \mathcal{H}_2$ describing the state of two quantum systems. If ρ is entangled, then there exists a Hermitian operator W acting on $\mathcal{H}_1 \otimes \mathcal{H}_2$ such that

$$\text{Tr}(W\rho) < 0 \text{ and } \text{Tr}(W\rho_{\text{sep}}) \geq 0 \tag{1.47}$$

for all separable density matrices ρ_{sep}.

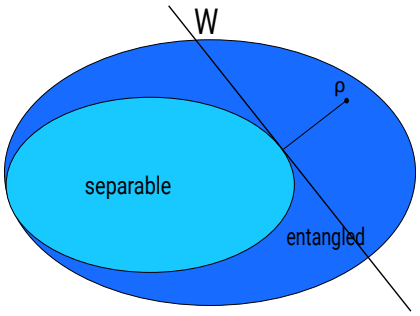

Figure 1.4: Schematic representation of the Hilbert space and a witness operator (from [14]). A witness can be understood as a hyperplane in the state space such that all separable states are on one side of the hyperplane. Hence, finding a state on the other side indicates entanglement. The opposite, however, does not hold.

Figure 1.4 illustrates this theorem. A hyperplane separating the set of all separable density matrices on $\mathcal{H}_1 \otimes \mathcal{H}_2$ can be defined from the point ρ. The hyperplane consists of a set of density matrices, κ, and its normal vector W is defined by $\mathrm{Tr}(W\kappa) = 0$. So the space is divided into two areas: in the first one, $\mathrm{Tr}(W\rho) \geq 0$ holds. All separable states will be found here together with some entangled states. In the second area, where $\mathrm{Tr}(W\rho) < 0$, no separable states will be found. As a consequence, the Terhal theorem provides a sufficient condition for the state ρ to be entangled. Given an proper entanglement witness W, if $\mathrm{Tr}(W\rho) < 0$ holds, ρ is an entangled state, as all separable (i.e., non-entangled states) give $\mathrm{Tr}(W\rho) \geq 0$. Please keep in mind that this is not a necessary condition. $\mathrm{Tr}(W\rho) \geq 0$ does not indicate that the state is separable. Possibly, the witness is just not suitable for that particular state, see Fig. 1.4.

The Terhal theorem can be used to construct an optimal witness given a theoretical state, for which the witness will be optimized. It can be shown that an optimal witness operator[5] W, which fulfills the Terhal Theorem, is given by

$$W = (|e_{min}\rangle \langle e_{min}|)^{T_a} \tag{1.48}$$

where $|e_{min}\rangle$ is the eigenvector of ρ^{T_a} corresponding to the smallest eigenvalue λ_{min} with $\lambda_{min} < 0$.

Calculating this explicitly for the Bell states one finds the following witness operators

$$\begin{aligned}
W(\phi^+) &= \frac{1}{2}(-|HH\rangle\langle VV| - |VV\rangle\langle HH| + |HV\rangle\langle HV| + |VH\rangle\langle VH|),\\
W(\phi^-) &= \frac{1}{2}(\ \ |HH\rangle\langle VV| + |VV\rangle\langle HH| + |HV\rangle\langle HV| + |VH\rangle\langle VH|),\\
W(\psi^+) &= \frac{1}{2}(\ \ |HH\rangle\langle HH| + |VV\rangle\langle VV| - |HV\rangle\langle VH| - |VH\rangle\langle HV|),\\
W(\psi^-) &= \frac{1}{2}(\ \ |HH\rangle\langle HH| + |VV\rangle\langle VV| + |HV\rangle\langle VH| + |VH\rangle\langle HV|).
\end{aligned} \tag{1.49}$$

If you apply the entanglement witness method to prove entanglement of the experimentally prepared states, evaluate the expectation value of the proper operator with respect to the measured state.

For our experimental situation where we produce a rather pure state, e.g., $|\phi^+\rangle$, it is always possible to find an optimal witness operator. However, in general, it is very hard to create, maintain, and manipulate entangled states under laboratory conditions. In fact, any system is usually subjected to the effects of external noise and interactions with the environment. These effects may turn pure states into mixed state. In this theoretical model, the noise is represented by a mixed state χ and the effectively produced state could be described by

$$\rho = p\,|\phi^+\rangle\langle\phi^+| + (1-p)\chi, \tag{1.50}$$

[5] A witness W is called optimal if there is no other witness that can detect more entangled states than W.

where p is the probability of having produced the desired state $|\phi^+\rangle$. Assuming that χ is white noise, the probability p is given by

$$p = \frac{1}{3}(1 - 4\,\mathrm{Tr}(W\rho)). \tag{1.51}$$

This probability can be considered as a measure for the entanglement quality of the state for which the witness was optimized.

Please note that a Bell inequality can also be seen as an entanglement witness, but it corresponds to a witness which is not optimized (for detecting entanglement). For the Bell states this means no difference, because they maximally violate a Bell inequality. However, there exist non-separable states which don't violate the Bell inequality, but their entanglement can be detected by a witness [14].

2 Experimental setup

In this part, the experimental implementation used in our case will be explained. The polarization degree of freedom is probably the most illustrative and most popular encoding of entanglement. Here we address the question of how to prepare and analyze a polarization-entangled state.
Figure 2.1 shows an overview of the experimental setup. It is split into two parts, first the generation of entangled photons in figure 2.1(a) and second the polarization analysis and the detection system in figure 2.1(b). These parts will be explained in detail in the following sections.

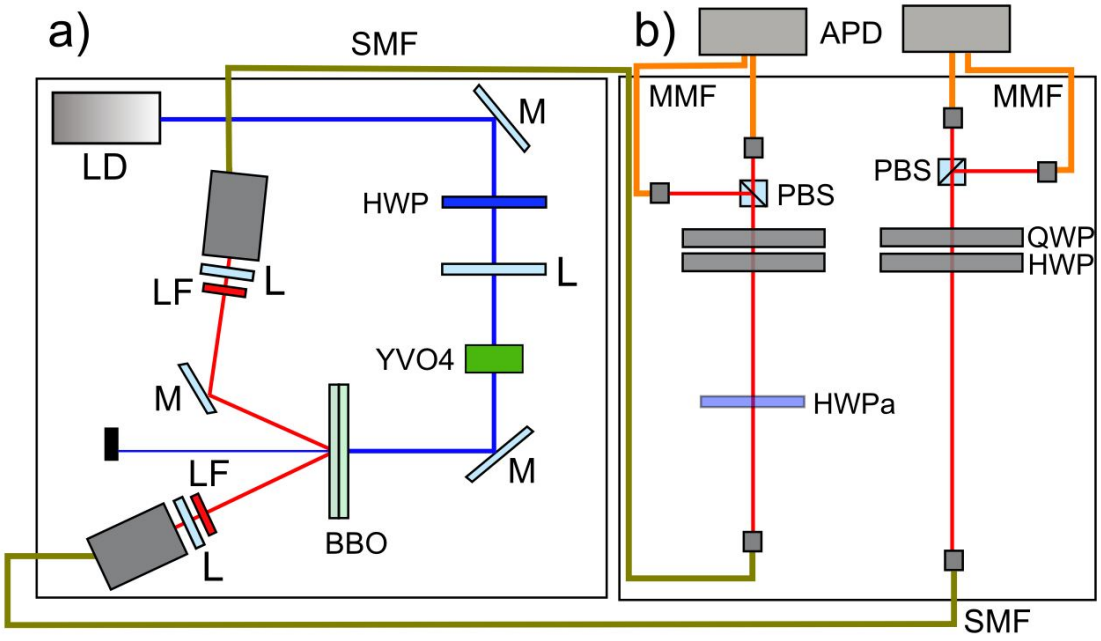

Figure 2.1: Schematic setup: laser diode (LD), longpass filter (LF), half-wave plate (HWP), lens (L), compensation crystal (YVO4), mirror (M), SPDC crystal (BBO), single-mode fiber (SMF), additional half-wave plate (HWPa), polarization beam splitter (PBS), multimode fiber (MMF),single photon detectors (APD).

2.1 Generation of the entangled photons

The pump laser - a UV laser diode

In the experiment a blue laser diode is used which produces vertical (V) polarized photons at nominal wavelength of $\lambda = 403\,\text{nm}$. It is driven with a supply current of up to 60 mA for which the optical output power is about 30 mW. The coherence length of the laser diode is in the range of some μm [27]. Using this laser, photon pairs produced by SPDC can be created.

SPDC with two BBO crystals

A single pump photon of the laser can be split up into a photon pair. Here we make use of a parametric process in nonlinear crystals, the Spontaneous Parametric Down Conversion (SPDC) [3]. The process can be explained by the presence of an electromagnetic field $\vec{E}$ in a crystal which induces a polarization $\vec{P}$ of the medium. In an anisotropic crystal, whereupon the relation between $\vec{P}$ and $\vec{E}$ depends on the direction of the latter, the components P_i of the polarization can be expressed in a power series

$$P_i = \epsilon_0 \sum_j \chi_{ij}^{(1)} E_j + \epsilon_0 \sum_{j,\,k} \chi_{ijk}^{(2)} E_j E_k + \dots \tag{2.1}$$

with $i, j, k \in \{\text{X,Y,Z}\}$ and ϵ_0 is the vacuum permittivity. $\chi_{ij}^{(1)}$ is the susceptibility tensor of the medium and $\chi_{ijk}^{(2)}$ its pendant of second order. Their typical strengths are in the range of $\chi_{ij}^{(1)} \approx 1$, $\chi_{ijk}^{(2)} \approx 10^{-10}$ cm/V [6]. So the second order can be neglected for weak fields, but a strong pump field is sufficient to generate a measurable result on the second order term of the polarization. In this picture the SPDC corresponds to the generation of two fields, called signal and idler, with the frequencies ω_s and ω_i out of one field with the frequency ω_p.
However, the SPDC can only be understood quantum mechanically as it represents a spontaneous process. In the photon picture it can be seen as the spontaneous conversion of a pump photon with energy $\hbar\omega_p$ and momentum $\hbar\vec{k}_p$ into two photons with energies $\hbar\omega_s$, $\hbar\omega_i$ and momenta $\hbar\vec{k}_s$, $\hbar\vec{k}_i$ [27].
In the SPDC process the energy and momentum conservation must hold,

$$\omega_p = \omega_s + \omega_i, \tag{2.2}$$

$$\vec{k}_p = \vec{k}_s + \vec{k}_i. \tag{2.3}$$

A more detailed quantum mechanical derivation of this process can be found in, e.g., [31]. When the pump beam is extraordinarily polarized, due to the birefringence of the optical material two types of SPDC can be distinguished[6]:

- **Type I**: Both down converted photons are ordinarily polarized regarding to the principal axis of the crystal.
- **Type II**: Signal and idler photons are orthogonally polarized, i.e., one is ordinarily, the other one extraordinarily polarized.

For exploiting the correlations in the polarization degree of freedom, two type-I nonlinear crystals made of Beta-barium borate (BBO) are used in this experiment [18]. These crystals are optically contacted, 1 mm thin and their optical axes lie in mutually perpendicular planes. For example, the optical axis of the first crystal is oriented along V, while for the second crystal it is orientated along H. Therefore, SPDC with a V-polarized pump beam occurs only in the first crystal, whereas with an H-polarized pump it occurs only

[6] Extraordinarily polarized means the polarization vector lies in the plane spanned by the principal axis of the crystal and the wave vector of the pump photon, in contrast to ordinarily polarized where the polarization vector is normal to this plane.

in the second crystal. By pumping the crystal with + (+ or P will be used as short-hand notation for polarization along +45° regarding to the H and V direction) polarized light the probability that a pump photon is down converted in either crystal is equal. As the initial state of +45° polarization is the coherent superposition of H and V polarization, both processes occur coherently. In order to prepare this initial polarization, an additional optical element (in our case a half-wave plate, see also section 2.2) is needed, which rotates the V polarized laser photons to + polarization.

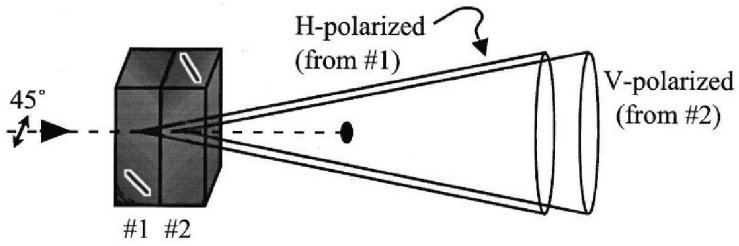

Figure 2.2: Two identical type I down-conversion crystals, oriented at 90° with respect to each other and the emission cones of the H and V polarized photons are illustrated (from [32]).

Momentum conservation implies that the down converted photons are emitted along symmetric cones around the pump beam direction. Furthermore, it imposes that correlated photon pairs can only be observed at diametrically opposed positions of the emission cones. In this double crystal type-I source the H-polarized photons lie on one cone and the V-polarized photons on the other cone [32]. Ideally, the two cones and, therefore, two photons in the $|HH\rangle$ or $|VV\rangle$ state overlap coherent at every point. To realize this experimentally, i.e., to prepare an entangled state out of the two photons, additional optical elements are needed. They will be described in the next sections.

Compensation and phase adjustment

Because of birefringence and chromatic dispersion in the optical material of the BBO crystals a temporal separation between the ordinarily and extraordinarily polarized photons arises. If the temporal separation is larger than the coherence time of the laser, no coherence between both photon pairs will be observed, as the photons can be distinguished in principle by their detection time. To solve this problem an additional compensation crystal is required. In this experiment a Yttrium Vanadate (YVO_4) crystal with an optical axis orientated parallel to the pump laser beam is introduced [26]. A variation of the optical path length and therefore a phase between the H and V components of the pump light can be implemented by tilting the crystal. So the time overlap between two photons of the SPDC processes can be adjusted and a high-quality entangled state can be produced.

Selection of two spatial modes

For the observation of a high quality entangled state the following points have to be considered. Lenses couple the photons into single mode fibers. They are placed at diametrically

opposed points of the emission cones. If they were not placed like this, no pairs of entangled photons could be detected (conservation of momentum). For a good state quality the two couplers collect the same amount of photons from both crystals [26].
Finally, spectral selection is achieved by introducing filters in each spatial selected mode centered around 805 nm with a bandwidth of about 6 nm. They are necessary, as the bandwidth of the down conversion photons is too wide to keep them indistinguishable due to different phases acquired in the fibers and in the optical components used to prepare and analyze the entangled state. But the disadvantage of these filters is the considerable reduction of the amount of produced photon pairs.

Preparation of Bell states

Like described above the source produces $|HH\rangle$ or $|VV\rangle$ photon states. After the alignment of the additional optical components, these pairs are in a coherent superposition and consequently the photons will automatically create the state

$$\begin{aligned} |\phi\rangle &= |H, A, E_1\rangle \otimes |H, B, E_2\rangle + \mathrm{e}^{i\phi} |V, A, E_1\rangle \otimes |V, B, E_2\rangle = \\ &= |A, B\rangle \ |E_1, E_2\rangle \ (|HH\rangle + \mathrm{e}^{i\phi} |VV\rangle). \end{aligned} \tag{2.4}$$

A and B correspond to the two spatially selected modes and E_1 and E_2 are the two energies of these modes. For a relative phase $\phi = 0$ (π) the Bell state $|\phi^+\rangle$ ($|\phi^-\rangle$) occur. The other two Bell states $|\psi^+\rangle$ and $|\psi^-\rangle$ can be prepared by adding a half-wave plate in one of the modes to exchange H and V polarization (for a detailed explanation see Sec. 2.2).
As a result of this process, two photonic qubits which differ in no other degree of freedom than their spatial mode and polarization can be generated very well (for details see [18]). The analysis of such a state will be explained in the following.

2.2 Polarization analysis and the detection system

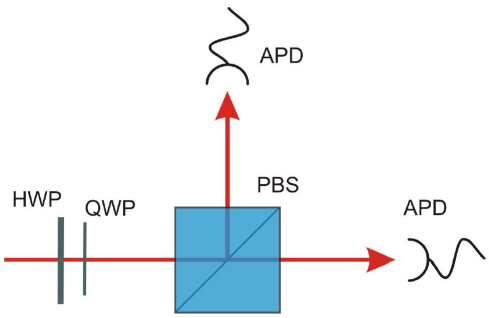

Figure 2.3: The polarization analysis as used in the experiment (from [5]).

Figure 2.3 shows the polarization analysis which is installed in each of the two spatial modes. Consequently, each photon is measured independently. The polarization analysis consists of a half-wave plate (HWP) and a quarter-wave plate (QWP) followed by a polarization beam splitter (PBS). The PBS transmits H-polarized and reflects V-polarized

light. In other words, the PBS implements a projection measurement onto the eigenvectors of σ_z, $|H\rangle$ and $|V\rangle$. To measure another polarization direction of the incoming photon, i.e., another vector of the Hilbert space, an additional rotation of the polarization direction onto H (or V) is necessary. This rotation is given by a HWP and a QWP.

The function of a HWP and a QWP can be summarized in the following way (see also [29]). Wave plates are implemented by zero-order, uniaxial birefringent crystals. A HWP introduces a relative phase shift of π between the ordinary and extraordinary polarization modes with respect to the orientation of the crystals. Hence, it rotates the polarization direction of linearly polarized light by an arbitrary angle, i.e., in the equatorial plane of the Bloch sphere (see figure 1.1). Accordingly, a QWP introduces a relative phase shift of $\frac{\pi}{2}$ and hence can transform linearly polarized light to circulary polarized light and vice versa. In the experiment the angles α_{HWP} and α_{QWP} between the vector of horizontal polarization and the principal axis of the wave plates can be set by a rotation of the wave plates.

Accordingly, it is possible to analyze any point on the Bloch sphere with these two wave plates. For example [3], when adjusting the HWP to $\alpha_{\mathrm{HWP}} = -\frac{\pi}{8}$ and the QWP to $\alpha_{\mathrm{QWP}} = 0$ an incoming photon in one of the eigenstates of $\widehat{\sigma}_x$, $|+\rangle$ or $|-\rangle$, is rotated to $|H\rangle$ or $|V\rangle$. In general, the wave plates rotate the eigenvectors of $\widehat{\sigma}_{\theta,\phi}$ onto the ones of $\widehat{\sigma}_z$ [6] according to

$$\widehat{\sigma}_z = (\mathrm{QWP}(\alpha_{\mathrm{QWP}})\,\mathrm{HWP}(\alpha_{\mathrm{HWP}}))\widehat{\sigma}_{\theta,\phi}(\mathrm{QWP}(\alpha_{\mathrm{QWP}})\,\mathrm{HWP}(\alpha_{\mathrm{HWP}}))^{\dagger} \tag{2.5}$$

$$\begin{aligned} \text{with} \quad \mathrm{HWP}(\alpha_{\mathrm{HWP}}) &= \begin{pmatrix} \cos(2\alpha_{\mathrm{HWP}}) & \sin(2\alpha_{\mathrm{HWP}}) \\ \sin(2\alpha_{\mathrm{HWP}}) & -\cos(2\alpha_{\mathrm{HWP}}) \end{pmatrix}, \\ \mathrm{QWP}(\alpha_{\mathrm{QWP}}) &= \begin{pmatrix} \cos^2(\alpha_{\mathrm{QWP}}) - i\sin^2(\alpha_{\mathrm{QWP}}) & (1+i)\cos(\alpha_{\mathrm{QWP}})\sin(\alpha_{\mathrm{QWP}}) \\ (1+i)\cos(\alpha_{\mathrm{QWP}})\sin(\alpha_{\mathrm{QWP}}) & -i\cos^2(\alpha_{\mathrm{QWP}}) + \sin^2(\alpha_{\mathrm{QWP}}) \end{pmatrix}. \end{aligned} \tag{2.6}$$

What angles α_{HWP} and α_{QWP} are needed to rotate a photon, which initially is (a) in the $|R\rangle$ or $|L\rangle$ and (b) in the state $|+\rangle$ or $|-\rangle$, to $|H\rangle$ or $|V\rangle$?

So far, single photon projections were described. For two photons, projections onto the two-qubit Hilbert space have to be associated to experimental values. The measurement of coincidences between two output modes correspond to a projection onto $|\uparrow\uparrow\rangle$, $|\uparrow\downarrow\rangle$, $|\downarrow\uparrow\rangle$ or $|\downarrow\downarrow\rangle$. A coincidence event means that we register two 'clicks' in two different detectors within a short (about 10 ns) time interval. The two outputs of each PBS are coupled into multi-mode fibers which are directed to single photon detectors (APDs). Their single photon sensitivity allows to trigger a single electrical pulse, when a photon is absorbed in the active semiconductor material. Two electrical pulses from different detectors are combined to measure coincidences [27].

The advantage of using a polarization analysis with two detectors in each mode is the possibility to detect simultaneously the four coincidence event numbers $C_{\uparrow\uparrow}$, $C_{\uparrow\downarrow}$, $C_{\downarrow\uparrow}$, $C_{\downarrow\downarrow}$.

These four numbers allow to determine the normalization of a state for each measurement setting, allowing to directly calculate the relative frequencies

$$f_{ij} = \frac{C_{ij}}{\sum_{i,j} C_{ij}} (i,j \in \{\uparrow,\downarrow\}). \tag{2.7}$$

They can be associated to the probabilities p_{ij} of Eqn.1.19. Therefore, the experimental measured correlations are given by

$$\begin{aligned} K_{ij}^{ex} &= f_{\uparrow\uparrow} - f_{\uparrow\downarrow} - f_{\downarrow\uparrow} + f_{\downarrow\downarrow} = \\ &= \frac{C_{\uparrow\uparrow}(\alpha_{\mathrm{HWP}},\alpha_{\mathrm{QWP}}) - C_{\uparrow\downarrow}(\alpha_{\mathrm{HWP}},\alpha_{\mathrm{QWP}}) - C_{\downarrow\uparrow}(\alpha_{\mathrm{HWP}},\alpha_{\mathrm{QWP}}) + C_{\downarrow\downarrow}(\alpha_{\mathrm{HWP}},\alpha_{\mathrm{QWP}})}{C_{\uparrow\uparrow}(\alpha_{\mathrm{HWP}},\alpha_{\mathrm{QWP}}) + C_{\uparrow\downarrow}(\alpha_{\mathrm{HWP}},\alpha_{\mathrm{QWP}}) + C_{\downarrow\uparrow}(\alpha_{\mathrm{HWP}},\alpha_{\mathrm{QWP}}) + C_{\downarrow\downarrow}(\alpha_{\mathrm{HWP}},\alpha_{\mathrm{QWP}})} \end{aligned} \tag{2.8}$$

with $i,j \in \{X,Y,Z\}$. A variation of the angles α_{HWP} and (α_{QWP}) allows to extract the correlation values for different bases.

Visibility

The visibility can be used to parameterize the contrast of measured graphs. The visibility of a function $\tilde{f}(\theta)$ is defined as

$$\mathcal{V} = \frac{\max_\theta(\tilde{f}(\theta)) - \min_\theta(\tilde{f}(\theta))}{\max_\theta(\tilde{f}(\theta)) + \min_\theta(\tilde{f}(\theta))}, \tag{2.9}$$

where max and min run over the angle θ. As a correlation function depending on an angle θ can be bounded between -1 and 1, calculating the visibility of this function in the given way would lead to $\mathcal{V} = \frac{2}{0}$.

Hence, we will make use of a suitable fit, allowing us to deduce the visibility of the correlation functions. For this purpose, find a proper fit function including a parameter $\mathcal{V}$ which can vary between 0 (for a flat line) and 1 (for a function which ranges from -1 to 1).

From clicks to density matrix

We have seen in section 1.3 that a density matrix of a two-qubit state can be written as

$$\rho = \frac{1}{4} \sum_{i,j=0}^{3} s_{ij}\, \widehat{\sigma}_i \otimes \widehat{\sigma}_j, \tag{2.10}$$

where the coefficients s_{ij} correspond to the K_{ij}^{ex}.

The sum contains 16 elements and, consequently, in principle 16 measurement values are needed to fully determine the density matrix of the state. The measurement of the whole set of two-photon projectors based on the Pauli matrices $\{\sigma_x, \sigma_y, \sigma_z\}$ requires 9 different settings. From these measurement 36 independent parameters can be extracted, i.e., the density matrix is over-determined.

The advantage of this method is that we can use the additional measurement results to obtain a better sensing of the state. For the calculation of the density matrix out of the experimental data, Eqn.2.10 can be expanded to

$$\begin{aligned}\rho &= \frac{1}{4}\sum_{i,j=0}^{3} K_{ij}^{ex}\ \widehat{\sigma}_i \otimes \widehat{\sigma}_j = \\ &= \frac{1}{4}(K_{00}\ (\mathbb{1}\otimes\mathbb{1}) + \sum_{i=1}^{3} K_{i0}^{ex}\ (\widehat{\sigma}_i\otimes\mathbb{1}) + \sum_{j=1}^{3} K_{0j}^{ex}\ (\mathbb{1}\otimes\widehat{\sigma}_j) + \sum_{i,j=1}^{3} K_{ij}^{ex}\ (\widehat{\sigma}_i\otimes\widehat{\sigma}_j)).\end{aligned} \tag{2.11}$$

K_{00} is set to 1 due to the normalization. Then, three different kinds of correlations appear in this expression. K_{ij}^{ex} are the above mentioned correlations, which are often called "full correlations" as they involve both parties' measurement results. K_{i0}^{ex} and K_{0j}^{ex} correspond to a local measurement, defined by tracing over the corresponding other qubit. That is why each local correlation can be extracted by an average over three measurements [5]. For example, the K_{01}^{ex} corresponds to an average over three measurements of the basis settings XX, YX and ZX and they can be calculated via

$$\begin{aligned}K_{0j}^{ex} &= \frac{C_{\uparrow\uparrow} - C_{\uparrow\downarrow} + C_{\downarrow\uparrow} - C_{\downarrow\downarrow}}{C_{\uparrow\uparrow} + C_{\uparrow\downarrow} + C_{\downarrow\uparrow} + C_{\downarrow\downarrow}},\\ K_{i0}^{ex} &= \frac{C_{\uparrow\uparrow} + C_{\uparrow\downarrow} - C_{\downarrow\uparrow} - C_{\downarrow\downarrow}}{C_{\uparrow\uparrow} + C_{\uparrow\downarrow} + C_{\downarrow\uparrow} + C_{\downarrow\downarrow}}.\end{aligned} \tag{2.12}$$

Example

As an example let us consider the density matrix of the Bell state $|\psi^+\rangle = \frac{1}{\sqrt{2}}(|HV\rangle + |VH\rangle)$. The correlations of this theoretical state $|\psi^+\rangle$ are given in Tab. 2.2.

$K_{...}$	0	X	Y	Z
0	1	0	0	0
X	0	1	0	0
Y	0	0	1	0
Z	0	0	0	-1

For example, the theoretical correlation value of K_{XX} is 1, while $K_{X0} = 0$. According to Eqn. 2.11, we can now assemble the density matrix ρ by using the correlation values and evaluating the tensor product of the respective Pauli matrices. Finally, we find for the density matrix

$$\rho = |\psi^+\rangle\langle\psi^+| = \begin{pmatrix} 0 & 0 & 0 & 0 \\ 0 & 0.5 & 0.5 & 0 \\ 0 & 0.5 & 0.5 & 0 \\ 0 & 0 & 0 & 0 \end{pmatrix}. \tag{2.13}$$

2.3 Software for the measurements

For the experiment, a measurement script is needed which is found in the directory '~/Praktikum/Messskript/'. The program exists in different version for the integration times and is started with a bash command ('./readcounts10Secs' or './readcounts60Secs'). It is used for getting the measurement results. For this purpose it integrates the coincidence count rates over a certain time period. The program returns the number of down-down coincidences (dd corresponding to $\downarrow\downarrow$), down-up (du, $\downarrow\uparrow$), up-down (ud, $\uparrow\downarrow$), and up-up (uu, $\uparrow\uparrow$). For measurements in ZZ basis, they directly correspond to HH, HV, VH, and VV coincidences, so please use the data of the four rows dd, du, ud, and uu.

3 Experimentation

Please read the following section carefully before starting with the experiment. The section *Experiments* contains some questions marked with the ▶-symbol. Please think about those beforehand.

Please pay attention to the following issues

- Never experiment without laser protection glasses. Already low intensities can harm your eyes permanently. The intensity of the laser beam is several orders of magnitude higher than the level for which a damage is probable.
- The used laser diode can be destroyed very easily by electrostatic discharging (ESD). So please do not touch either the laser diode or the cables and avoid electrostatically charging yourself.
- Take care of the optical components. Please do not touch any surfaces of the lenses, the waveplates or the mirrors.
- Pay particular attention to the fiber optics. Do not touch them and do not put anything on them or on the two breadboards. Otherwise, the polarization of the photons can be changed.
- Pay attention to the respective angle offsets of the waveplates. To compensate for the offset due to their mounting, all waveplates are labelled to indicate their 0° position. Add this given angle offset to the desired angle position.

Alignment

The alignment of the single components is already done and will be described in detail by the tutor. Before the measurement,

- the optomechanical components for coupling the down conversion photons to the single mode fiber optics,
- YVO_4-crystal to align the phase, and
- the optical fibers to maintain the polarization

had to be adjusted. Please do not change down-conversion setup itself or touch the fiber optics.

Experiments

1. **Measuring the correlation function**
   In this experiment two correlation functions will be detected. For the first measurement run, one HWP is set to 0° and the other HWP is rotated from 0° to 90° in small steps. For the second run, one HWP is set to 22.5°, while the other is again rotated from 0° to 90°.
   ▶ *Why are measurements of correlation functions in two bases necessary to prove entanglement?*

2. **Bell Inequality**
   In this setup (corresponding to the physical situation described in section 1.2.2-Quantum violation) a violation of the CHSH inequality can be obtained when setting the HWPs according to the following table.

Alice		Bob	
α	α'	β	β'
22.5°	0°	11.25°	-11.25°

   ▶ *Why are those measurement angles suitable for a violation of the CHSH inequality?*

   Set the HWPs to each of the four combinations of Alice's and Bob's angles (α, β; α, β'; α', β; and α', β'). Measure with an integration time of 60 s.

3. **Quantum Tomography** of $|\phi^+\rangle$
   Perform a quantum state tomography of the given state $|\phi^+\rangle$. The following table summarizes how to set the waveplates for the respective measurements.

all in °		HWP A	QWP A	HWP B	QWP B
X	X	22.5	0	22.5	0
X	Y	22.5	0	0	45
X	Z	22.5	0	0	0
Y	X	0	45	22.5	0
Y	Y	0	45	0	45
Y	Z	0	45	0	0
Z	X	0	0	22.5	0
Z	Y	0	0	0	45
Z	Z	0	0	0	0

4. **Rotate the state to** $|\phi^-\rangle$
   To change the state from $|\phi^+\rangle$ to $|\phi^-\rangle$, put a HWP in front of Alice's polarization analysis (PA).
   ▶ *What angle* α_{HWP} *is needed for this purpose?*
   ▶ *What is the transformation of that waveplate?*
   Measure the density matrix of this state.

5. **Rotate the state to** $|\psi^+\rangle$
   Put a HWP in one mode in front of Bob's PA to rotate from $|H\rangle$ to $|V\rangle$ and from $|V\rangle$ to $|H\rangle$.
   ▶ *What angle* α_{HWP} *is needed for this purpose?*
   Measure the density matrix of this state.

6. **Rotate the state to** $|\psi^-\rangle$
   Use two HWP in order to prepare $|\psi^-\rangle$.
   ▶ *How do the HWPs have to be set?*
   Measure the density matrix of this state.

To check during your measurements if you had prepared the correct state, you can compare your measured relative frequencies of the four coincidences with the following table. This schematic diagram shows the relative frequencies of the ↑↑, ↑↓, ↓↑ and ↓↓ coincidences of the four Bell states for measuring XX, YY and ZZ. When performing any other measurement (e.g., XY, ZX, etc.), all four coincidence channels should give roughly the same amount of counts, leading to relative frequencies of 0.25 for all.

	XX	YY	ZZ
ϕ^+	.5 0 0 .5	0 .5 .5 0	.5 0 0 .5
ψ^+	.5 0 0 .5	.5 0 0 .5	0 .5 .5 0
ψ^-	0 .5 .5 0	0 .5 .5 0	0 .5 .5 0
ϕ^-	0 .5 .5 0	.5 0 0 .5	.5 0 0 .5

4 Evaluation

Your report should describe at least

- the generation of entangled photons,
- the experimental setup,
- the characteristical features of qubits and entanglement, and
- the basics of quantum tomography.

With regard to the measurements, please

- discuss the measured correlation functions and answer the question why two correlation functions are necessary for entanglement detection. Calculate for each of the two correlation functions the visibility by using a suitable fit as described above (section 2.2-'visibility').
- Show the violation of the Bell inequality with a calculation of errors using error propagation. For that, you can assume a) that the coincidences follow Poissonian distributions (allowing you to estimate an error for the measured coincidence counts) and b) that the total number of coincidences is constant and hence without an error. Interpret your result.
- Evaluate the density matrices of the four produced states and discuss the results, i.e., calculate the fidelity with respect to the corresponding ideal state, compute the purity, prove entanglement (for at least one of the four states) with both methods introduced in sec. 1.3.2 and calculate and discuss the eigenvalues of the reconstructed states.

References

[1] Claude Cohen-Tannoudji, Bernard Diu, and Franck Laloe. *Quantum mechanics*. Wiley, 1977.

[2] Michael A. Nielsen and Isaac L. Chuang. *Quantum computation and quantum information*. Cambridge University Press, 2000.

[3] Christian I. T. Schmid. *Multi-photon entanglement and applications in quantum information*. PhD thesis, LMU München, 2008.

[4] Jügen Volz. *Atom-Photon Entanglement*. PhD thesis, LMU München, 2006.

[5] Nikolai Kiesel. *Experiments on Multiphoton Entanglement*. PhD thesis, LMU München, 2007.

[6] Witlef Wieczorek. *Multi-Photon Entanglement*. PhD thesis, LMU München, 2009.

[7] Albert Einstein, Boris Podolsky, and Nathan Rosen. Can Quantum-Mechanical Description of Physical Reality Be Considered Complete? *Phys. Rev.*, 47(10):777–780, May 1935.

[8] Achim Beetz. Die Bellschen Ungleichungen, 2005.

[9] M.O. Scully and M.S. Zubairy. *Quantum optics*. Cambridge University Press, 1997.

[10] Erwin Schrödinger. Die gegenwärtige Situation in der Quantenmechanik. *Naturwissenschaften*, 23:807–812, 1935.

[11] John S. Bell. On the Einstein-Podolsky-Rosen paradox. *Physics*, 1:195–200, 1964.

[12] Dieter Meschede. *Optik, Licht und Laser*. Teubner Studienbuecher. Teubner, 2005.

[13] John F. Clauser, Michael A. Horne, Abner Shimony, and Richard A. Holt. Proposed Experiment to Test Local Hidden-Variable Theories. *Phys. Rev. Lett.*, 23(15):880–884, Oct 1969.

[14] Carsten Schuck. Experimental Implementation of a Quantum Game. Diplomarbeit, LMU München, 2003.

[15] Stuart J. Freedman and John F. Clauser. Experimental Test of Local Hidden-Variable Theories. *Phys. Rev. Lett.*, 28(14):938–941, Apr 1972.

[16] Alain Aspect, Philippe Grangier, and Gérard Roger. Experimental Tests of Realistic Local Theories via Bell's Theorem. *Physical Review Letters*, 47:460–463, 1981.

[17] Alain Aspect, Jean Dalibard, and Gérard Roger. Experimental Test of Bell's Inequality Using Time-Varying Analyzers. *Physical Review Letters*, 49:1804–1807, 1982.

[18] Pavel Trojek. *Effcient Generation of Photonic Entanglement and Multiparty Quantum Communication*. PhD thesis, LMU München, 2007.

[19] Gregor Weihs, Thomas Jennewein, Christoph Simon, Harald Weinfurter, and Anton Zeilinger. Violation of Bell's Inequality under Strict Einstein Locality Conditions. *Phys. Rev. Lett.*, 81(23):5039–5043, Dec 1998.

[20] Thomas Scheidl, Rupert Ursin, Johannes Kofler, Sven Ramelow, Xiao-Song Ma, Thomas Herbst, Lothar Ratschbacher, Alessandro Fedrizzi, Nathan Langford, Thomas Jennewein, and Anton Zeilinger. Violation of local realism with freedom of choice. 2010.

[21] B. Hensen, H. Bernien, A.E. Dréau, A. Reiserer, N. Kalb, M.S. Blok, J. Ruitenberg, R.F.L. Vermeulen, R.N. Schouten, C. Abellán, W. Amaya, V. Pruneri, M.W. Mitchell, M. Markham, D.J. Twitchen, D. Elkouss, S. Wehner, T.H. Taminiau, and R. Hanson. Loophole-free Bell Inequality Violation Using Electron Spins Separated By 1.3 Kilometers. *Nature (London)*, 526:682–686, Oct 2015.

[22] Marissa Giustina, Marijn A. M. Versteegh, Sören Wengerowsky, Johannes Handsteiner, Armin Hochrainer, Kevin Phelan, Fabian Steinlechner, Johannes Kofler, Jan-Åke Larsson, Carlos Abellán, Waldimar Amaya, Valerio Pruneri, Morgan W. Mitchell, Jörn Beyer, Thomas Gerrits, Adriana E. Lita, Lynden K. Shalm, Sae Woo Nam, Thomas Scheidl, Rupert Ursin, Bernhard Wittmann, and Anton Zeilinger. Significant-Loophole-Free Test of Bell's Theorem with Entangled Photons. *Phys. Rev. Lett.*, 115:250401, Dec 2015.

[23] Lynden K. Shalm, Evan Meyer-Scott, Bradley G. Christensen, Peter Bierhorst, Michael A. Wayne, Martin J. Stevens, Thomas Gerrits, Scott Glancy, Deny R. Hamel, Michael S. Allman, Kevin J. Coakley, Shellee D. Dyer, Carson Hodge, Adriana E. Lita, Varun B. Verma, Camilla Lambrocco, Edward Tortorici, Alan L. Migdall, Yanbao Zhang, Daniel R. Kumor, William H. Farr, Francesco Marsili, Matthew D. Shaw, Jeffrey A. Stern, Carlos Abellán, Waldimar Amaya, Valerio Pruneri, Thomas Jennewein, Morgan W. Mitchell, Paul G. Kwiat, Joshua C. Bienfang, Richard P. Mirin, Emanuel Knill, and Sae Woo Nam. Strong Loophole-Free Test of Local Realism. *Phys. Rev. Lett.*, 115:250402, Dec 2015.

[24] Wenjamin Rosenfeld, Daniel Burchardt, Robert Garthoff, Kai Redeker, Norbert Ortegel, Markus Rau, and Harald Weinfurter. Event-Ready Bell Test Using Entangled Atoms Simultaneously Closing Detection and Locality Loopholes. *Phys. Rev. Lett.*, 119:010402, Jul 2017.

[25] Daniel F. V. James, Paul G. Kwiat, William J. Munro, and Andrew G. White. Measurement of qubits. *Phys. Rev. A*, 64(5):052312, Oct 2001.

[26] Martin Schaeffer. Two-Photon Polarization Entanglement in Typ I SPDC Experiment. Bachelorthesis, LMU München, 2009.

[27] Christian I. T. Schmid. Kompakte Quelle verschränkter Photonen und Anwendungen in der Quantenkommunikation. Diplomarbeit, LMU München, 2004.

[28] Armin Uhlmann. The transition probability in the state space of a *-algebra. *Reports on Mathematical Physics*, 9:273–279, 1976.

[29] Joseph B. Altepeter, Daniel F. V. James, and Paul G. Kwiat. 4 Qubit Quantum State Tomography. *Representations*, 145:113–145, 2004.

[30] Otfried Gühne and Géza Tóth. Entanglement detection. *Physics Reports*, 474(1):1–75, 2009.

[31] Leonard Mandel and Emil Wolf. *Optical Coherence and Quantum Optics*, volume 64. Cambridge University Press, 1995.

[32] Paul G. Kwiat, Edo Waks, Andrew G. White, Ian Appelbaum, and Philippe H. Eberhard. Ultrabright source of polarization-entangled photons. *Phys. Rev. A*, 60(2):R773–R776, Aug 1999.